

Synthesis, Structure, and Properties of the New Mixed-Valent Dodecahalogenotrimetallate $\text{In}_4\text{Ti}_3\text{Br}_{12}$ and its Relation to Compounds $\text{A}_3\text{Ti}_2\text{X}_9$ ($\text{A} = \text{K}, \text{In}$; $\text{X} = \text{Cl}, \text{Br}$)

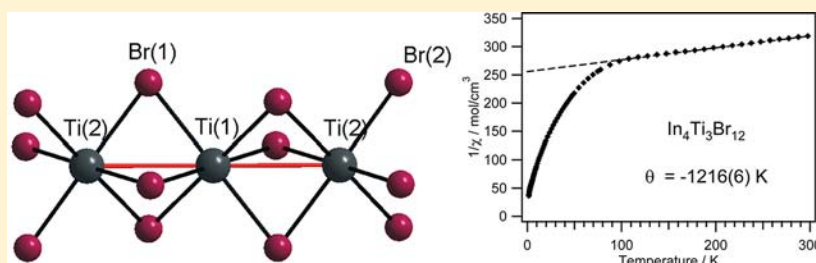
Melanie Schroeder,[†] Sabina Hartwig,[†] Karl W. Krämer,[‡] Silvio Decurtins,[‡] and Harald Hillebrecht^{*,†,§}

[†]Institut für Anorganische und Analytische Chemie, Albert-Ludwigs-Universität Freiburg, Albertstr. 21, D-79104 Freiburg, Germany

[‡]Departement für Chemie und Biochemie, Universität Bern, Freiestr. 3, CH-3012 Bern, Switzerland

[§]Freiburger Materialforschungszentrum FMF, Stefan-Maier-Str. 25, D-79104 Freiburg, Germany

Supporting Information



ABSTRACT: Black single crystals of the new dodecahalogenotrimetallate $\text{In}_4\text{Ti}_3\text{Br}_{12}$ were obtained by reacting InBr_3 with Ti-wire at 450 °C in a silica tube sealed under vacuum. $\text{In}_4\text{Ti}_3\text{Br}_{12}$ (Pearson symbol $hR57$, space group $R\bar{3}m$, $Z = 3$, $a = 7.3992(8)$ Å, $c = 36.673(6)$ Å, 643 refl., 25 param., $R_1(F) = 0.025$; $wR_2(F^2) = 0.046$) is a defect variant of a 12 L-perovskite. In^+ cations are 12-fold coordinated in two different ways: In1 as an anticuboctahedron and In2 as a cuboctahedron. In both cases the $5s^2$ configuration results in 3 short, 6 medium, and 3 long In–Br distances which might be explained as lone pair effect or second order Jahn–Teller instability. Furthermore there are isolated linear trimers $[\text{Ti}_3\text{Br}_{12}]^{4-}$ consisting of facesharing octahedra similar to $[\text{Ru}_3\text{Cl}_{12}]^{4-}$. The $[\text{Ti}_3\text{Br}_{12}]^{4-}$ -unit has to be described as a mixed-valent d^1 - d^2 - d^1 system. According to magnetic measurements, the Ti-atoms in $\text{In}_4\text{Ti}_3\text{Br}_{12}$ show strong antiferromagnetic interactions ($\Theta = -1216(6)$ K) which might be addressed as weak Ti^{3+} – Ti^{2+} – Ti^{3+} bonds. For comparison, single crystals of $\text{K}_3\text{Ti}_2\text{X}_9$ ($\text{X} = \text{Cl}, \text{Br}$) were synthesized and their structures refined. The rotation of the $\text{Ti}_2\text{X}_9^{3-}$ dimers reduced the symmetry of the well-known $\text{Cs}_3\text{Cr}_2\text{Cl}_9$ type from $P6_3/mmc$ to $P6_3/m$ and resulted in the formation of merohedral twins. According to the unit cell volumes In^+ is smaller than K^+ in all cases.

INTRODUCTION

Ternary halides $\text{A}_x\text{M}_y\text{X}_z$ of transition metals (M) with monovalent cations $A = \text{K}, \text{Rb}, \text{Cs}, \text{In}, \text{Tl}$ and halides $X = \text{Cl}, \text{Br}, \text{I}$ represent a large family of compounds. When A and X are present in a 1:3 ratio they form a closest sphere packing and the M^{n+} cations ($n = 2, 3, 4$) occupy octahedral (and in a few cases tetrahedral) voids formed by X . Among them those with titanium as the transition metal and indium as the monovalent cation are of special interest because of four reasons.

(1) Titanium can occur in these compounds in oxidation states +2, +3, and +4. An example is the series CsTiCl_3 (hexagonal perovskite, BaNiO_3 structure^{1,2}), $\text{Cs}_3\text{Ti}_2\text{Cl}_9$ ($\text{Cs}_3\text{Cr}_2\text{Cl}_9$ structure³), and Cs_2TiCl_6 (K_2PtCl_6 structure^{1,2}).

(2) Titanium halides show a remarkable tendency to form compounds of mixed valence. Recently, Meyer et al. have given an excellent review on Ti halides.⁴

(3) The Ti^{3+} (d^1) and Ti^{2+} (d^2) compounds with condensed TiX_6 -octahedra are model systems for the investigation of Ti–Ti interactions.^{5–9}

(4) In^+ represents a ns^2 cation which shows the “lone pair/inert pair phenomenon”. In a recent review Pardoe and

Downs¹⁰ pointed out that the number of $\text{In}(\text{I})$ compounds with appreciable ionic character is still very limited.

Our interest in $\text{A}_3\text{M}_2\text{X}_9$ compounds started when we investigated trihalides with chain structure MX_3 ($M = \text{Mo}, \text{Ru}$; $X = \text{Br}, \text{I}$)^{11,12} as representatives of one-dimensional (1D) metals. The $\text{A}_3\text{M}_2\text{X}_9$ compounds contain dimers of facesharing octahedra, and the $[\text{M}_2\text{X}_9]^{3-}$ units can be used as model systems for the M – M interaction. For $M = \text{Mo}$ and Ru it turned out that the usual symmetry of the $\text{Cs}_3\text{Cr}_2\text{Cl}_9$ structure (i.e., $P6_3/mmc$) is sometimes reduced to $P6_3/m$ for compounds with $A = \text{K}$ and Tl . The reduced symmetry, that was already described for $\text{K}_3\text{W}_2\text{Cl}_9$,¹³ is due to a rotation of the $[\text{M}_2\text{X}_9]^{3-}$ unit, which might be caused by the small cation size of K^+ and Tl^+ . Subtle differences (i.e., $\text{K}_3\text{Mo}_2\text{Cl}_9$ and $\text{Tl}_3\text{Mo}_2\text{Cl}_9$ are distorted, $\text{K}_3\text{Ru}_2\text{Cl}_9$ and $\text{Tl}_3\text{Ru}_2\text{Cl}_9$ are not) led to the idea that the extent of the M – M interaction has an influence, too.⁵ Therefore, we extended our investigations on systems with

Received: May 8, 2012

Published: July 23, 2012

small A^+ cations (K^+) and only weakly interacting M^{3+} cations (Ti^{3+}).¹⁴

In the course of systematic studies on In^+ compounds Dronskowski¹⁵ described in 1995 $In_3Ti_2Br_9$ as the first representative of a ternary $In(I)$ – $Ti(III)$ halide. According to the single crystal X-ray investigation it belongs to the $Cs_3Cr_2Cl_9$ structure ($Z = 2$, $P6_3/mmc$). In contrast to other isostructural compounds the surrounding of In^+ was described as severely distorted in a $3 + 6 + 3$ manner. The displacement parameters were enlarged and one In^+ cation occupies a split site. This phenomenon was explained by Dronskowski as a second-order Jahn–Teller instability.

When it turned out that $K_3Ti_2Cl_9$ and $K_3Ti_2Br_9$ crystallize in space group $P6_3/m$ and the crystals of both compounds form merohedral twins which pretend the higher symmetry¹⁴ we decided to reinvestigate the structure of $In_3Ti_2Br_9$ with respect to the possibility of twinning. Furthermore, we have characterized the new compound $In_4Ti_3Br_{12}$. This is the first dodecahalogenotrimetallate with monovalent indium. It represents a defect 12 L-(or 12R-)perovskite structure in which the Ti-atoms occupy the octahedral voids of bromine atoms. The hexagonal layer sequences contain isolated $[Ti_3Br_{12}]^{4-}$ trimers consisting of face-sharing $TiBr_6$ -octahedra. These structural units are very rare but also known in the mixed-valent anion $[Ru_3Cl_{12}]^{4-}$.¹⁶ The Mo(III)-compound $[Mo_3Cl_{12}]^{3-}$ was concluded from conductivity measurement and spectroscopic data.¹⁷ Later on the analogous anions $[Mo_3I_{12}]^{3-}$ and $[Mo_3Br_{12}]^{3-}$ were characterized and $(PPH_4)_3[Mo_3I_{12}]$ confirmed by an X-ray crystal structure analysis.¹⁸ Furthermore, calculations on electronic structure and M – M interactions were done by Stranger et al.¹⁹ Very recently Meyer et al. gave a short communication on the structurally closely related but monoclinic $K_4Ti_3Br_{12}$.²⁰

To discuss the different aspects (twinning, Ti–Ti interaction, size of In^+) we present our results on $K_3Ti_2Cl_9/K_3Ti_2Br_9$ and $In_4Ti_3Br_{12}$ in one contribution.

EXPERIMENTAL SECTION

Synthesis and Characterization. $K_3Ti_2Cl_9/K_3Ti_2Br_9$. The synthesis of ternary halides of titanium and alkali metals A can follow three different routes. First, the appropriate binary Ti-halide TiX_n is combined with AX . Second, titanium metal, the halogen, and AX are reacted. Or third, AX , titanium metal, and a higher-valent Ti-halide are used. For $X = Cl$ we followed the first route, for $X = Br$ the third one. The educts (total mass ca. 500 mg) were sealed in a silica tube (diameter 10 mm, length 6 cm) and submitted to the following temperature program (heating/cooling rates in italics, dwelling time in brackets):

$K_3Ti_2Cl_9$. RT 1 K/min, 700 °C (38 d); 0.1 K/h, 350 °C (1 d); 0.2 K/h, RT.

$K_3Ti_2Br_9$. RT 0.1 K/min 120 °C (2 h); 0.2 K/min 150 °C (6 h); 0.2 K/min 185 °C (12 h); 0.2 K/min 300 °C (5 d); 0.2 K/min 400 °C (1 d); 0.2 K/min 500 °C (1 d); 0.2 K/min 800 °C (10 d); 0.1 K/h 350 °C (7 d); 0.5 K/h RT.

The XRD powder patterns were completely indexed with the hexagonal unit cell of the $K_3W_2Cl_9$ structure. Observed intensities were in agreement to those calculated from the structural parameters. Reflections violating the condition for the glide plane (hhl with $l = 2n + 1$) were not observed because of its low intensity and the poor quality of the diffraction patterns.

$In_4Ti_3Br_{12}/In_3Ti_2Br_9$. For the synthesis of $In_4Ti_3Br_{12}$ Ti-wire and $InBr_3$ (1:1) were reacted in an evacuated silica ampule at 450 °C for 5 days and then the furnace was turned off. The only crystalline products were black hexagonal platelets ($\varnothing_{max} = 0.4$ mm, Figure 1), which grew

grape-like on the surface of the Ti-wires. A molten regulus was observed at the bottom of the silica tube.



Figure 1. Crystals of $In_4Ti_3Br_{12}$ formed on a Ti-wire.

From powder diffraction patterns the black lustrous crystals were identified as phase pure $In_4Ti_3Br_{12}$. The regulus remaining after the synthesis consists of $In_3Ti_2Br_9$ (see Figure 2).

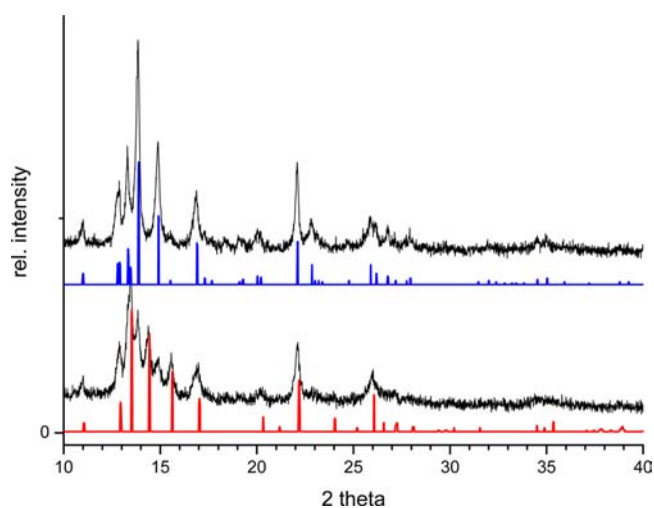


Figure 2. X-ray powder diffraction patterns of regulus (top) and selected crystals (bottom) from the $In_4Ti_3Br_{12}$ synthesis. Calculated patterns are shown as line bars. The lower diagram contains only $In_4Ti_3Br_{12}$, the upper diagram additional $In_3Ti_2Br_9$.

Structure Solution and Refinements. All single crystals were sensitive to moisture and air. Therefore, they were handled in an argon-filled glovebox. For the measurements suitable single crystals were mechanically isolated from the solidified melt and fixed in a silica glass capillary. Measurements were performed at room temperature with graphite-monochromated Mo– $K\alpha$ -radiation ($\lambda = 0.71073$ Å) using a single crystal diffractometer STOE IPDS I ($K_3Ti_2Cl_9$, $K_3Ti_2Br_9$) or IPDS II ($In_3Ti_2Br_9$, $In_4Ti_3Br_{12}$) equipped with an image plate detector. Corrections (Lorentz, polarization), data reduction, and determination of lattice parameters were done with the program XAREA.²¹ A numerical absorption correction was applied using the equivalent method (Program XSHAPE²¹). Refinements were done with SHELXTL.²²

$K_3Ti_2Cl_9/K_3Ti_2Br_9$. For both compounds (Figure 3) the indexing routine led to a hexagonal unit cell of the $Cs_3Cr_2Cl_9$ -type. The refinement with this structure model resulted in unsatisfying R -factors ($K_3Ti_2Cl_9$: $R_1 = 0.15$, $wR_2 = 0.33$; $K_3Ti_2Br_9$: $R_1 = 0.20$, $wR_2 = 0.60$). The displacement parameters for potassium ($K_3Ti_2Br_9$) and chloride ($K_3Ti_2Cl_9$) were enlarged and the reflection condition hhl with $l = 2n$ violated. According to the experience with $K_3Mo_2Br_9$ and $K_3Ru_2Br_9$ the symmetry was lowered to $P6_3/m$ and a merohedral twinning assumed. This improved the refinement significantly. Twinning ratios

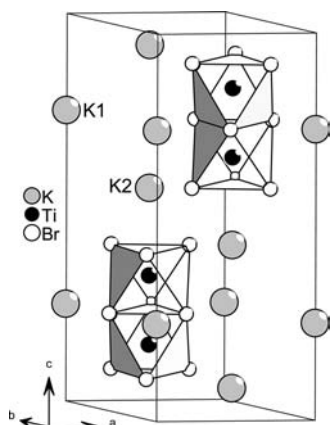


Figure 3. Crystal structure of $K_3Ti_2Br_9$.

were 69.5(3)% ($K_3Ti_2Cl_9$) and 63(1)% ($K_3Ti_2Br_9$), respectively. Details of the final refinements are given in Tables 1, 2 and as Supporting Information.

$In_4Ti_3Br_{12}$. One of the small black hexagonal platelets (diameter 0.4 mm, thickness 0.2 mm) was selected under a microscope. The indexing routine led to a rhombohedral unit cell. Lattice parameters were refined from the data set²¹ to $a = 7.3992(8)$ Å and $c = 36.673(6)$ Å. Measurement of 6472 reflections up to $2\theta = 58^\circ$ and merging in Laue class $\bar{3}m$ resulted in a data set of 643 unique reflections (410 with $I > 2\sigma(I)$). Except for the reflection conditions for the rhombohedral crystal system (hkl with $-h + k + l = 3n$), no additional extinctions were found. The crystal structure was solved by direct methods²² in $R\bar{3}m$ and refined without peculiarities. A check of the symmetry and the following refinement showed that the structure is centrosymmetric

and $R\bar{3}m$ the correct space group. Finally $R_1(F) = 0.025$ and $wR_2(F^2) = 0.046$ were obtained.

Details of structure solutions and refinements are listed in Tables 1, 3, and the Supporting Information. Further details of the crystal structure investigations may be obtained from the Fachinformationszentrum Karlsruhe, D-76344 Eggenstein-Leopoldshafen (Germany) (fax: +49)724-808-666; e-mail: crysdata@fiz-karlsruhe.de) on quoting the depository numbers CSD-423119 ($K_3Ti_2Cl_9$), CSD 423120 ($K_3Ti_2Br_9$), and CSD-423124 ($In_4Ti_3Br_{12}$).

Magnetic Measurements. The magnetic susceptibility of $In_4Ti_3Br_{12}$ was measured on a Quantum Design MPMS SQUID in the temperature range from 1.8 to 300 K in a field of 500 Oe. A powder sample of 53.5 mg was sealed in a gelatin capsule in a drybox. The data were corrected for the diamagnetic contributions of the capsule and the sample diamagnetism of 5.54×10^{-4} emu/mol.

RESULTS AND DISCUSSION

$K_3Ti_2Cl_9$, $K_3Ti_2Br_9$. Both compounds belong to the symmetry-reduced $K_3W_2Cl_9$ structure¹³ which is closely related to the much more common $Cs_3Cr_2Cl_9$ structure.³ The $Cs_3Cr_2Cl_9$ structure can be described as a defect variant of a 6H-perovskite with a layer sequence ABACBC = (hcc)₂. According to the building principle of perovskite-related structures the big monovalent cations A^+ are of comparable size to the halide anions X^- . With an $A:X$ ratio of 1:3 they together form closest layers perpendicular to the c -axis. Within the hexagonal sequences the M^{3+} cations occupy the octahedral voids formed exclusively by the anions, while those in the cubic sequences remain empty. There are two independent A^+ cation sites both with coordination number 12: A1 in the hexagonal sequence ("anti"-cuboctahedron) and A2 in the cubic sequence (cuboctahedron). The most prominent structural feature are

Table 1. Crystal Data and Structure Refinements of $K_3Ti_2X_9$ ($X = Cl, Br$) and $In_4Ti_3Br_{12}$

compound	$K_3Ti_2Cl_9$	$K_3Ti_2Br_9$	$In_4Ti_3Br_{12}$
crystal shape	irregular fragment	irregular polyhedron	hexagonal platelet
size [mm ³]	0.08 × 0.08 × 0.15	0.05 × 0.05 × 0.05	0.1 × 0.1 × 0.05
crystal system	hexagonal	hexagonal	rhombohedral
space group	$P6_3/m$	$P6_3/m$	$R\bar{3}m$
formula units	$Z = 2$	$Z = 2$	$Z = 3$
unit cell [Å]	$a = 7.0733(14)$ $c = 17.544(5)$	$a = 7.429(3)$ $c = 18.382(9)$	$a = 7.3992(8)$ $c = 36.673(6)$
volume [Å ³]	$V = 760.14$	$V = 878.5$	$V = 1738.8$
$d_{calc.}$ [g/cm ³]	2.325	3.524	4.47
	$0^\circ \leq \omega \leq 180^\circ$ $\psi = 0^\circ, \Delta\omega = 2^\circ$	$0^\circ \leq \omega \leq 180^\circ$ $\psi = 0^\circ, \Delta\omega = 2^\circ$	$0^\circ \leq \omega \leq 180^\circ$ $\psi = 0^\circ, 111^\circ; \Delta\omega = 2^\circ$
exposure time/frame	240 s	600 s	720 s
θ range	$6.7^\circ < 2\theta < 50^\circ$ $-8 < h < 8$ $-8 < k < 8$ $-20 < l < 20$	$6.7^\circ < 2\theta < 50^\circ$ $-8 < h < 8$ $-8 < k < 8$ $-21 < l < 21$	$4^\circ < 2\theta < 58.5^\circ$ $-8 < h < 8$ $-8 < k < 8$ $-50 < l < 50$
μ [mm ⁻¹]	3.41	22.05	25.55
$R_{int.}/R_{sigma}$	0.060/0.029	0.203/0.067	0.073/0.034
$T_{min.}/T_{max}$	0.584/0.655	0.046/0.086	0.085/0.413
$N(hkl)$ meas.; unique	4529; 439	5595; 533	6472; 643
$N'(hkl)$ ($I > 2\sigma(I)$)	328	394	410
parameters refined	26	26	25
R -values $R_1(F)/wR_2(F^2)$	0.027/0.052	0.092/0.256	0.025/0.046
$R_1(F)$, all data	0.046	0.111	0.048
weighting scheme ¹⁶	0.0242/0.0	0.124/6.7	0.0212/0.0
extinction ¹⁶	0.0000(1)	0.0009(13)	0.0023(1)
goodness of fit	0.908	1.087	0.727
residual electron density in [$e^-/\text{Å}^3$] (max., min., σ)	+0.26/-0.23/0.06	+1.48/-0.94/0.24	+0.74/-0.96/0.12

Table 2. Unit Cell Parameters and Selected Distances (Å) and angles (deg) of $A_3Ti_2X_9$ Compounds

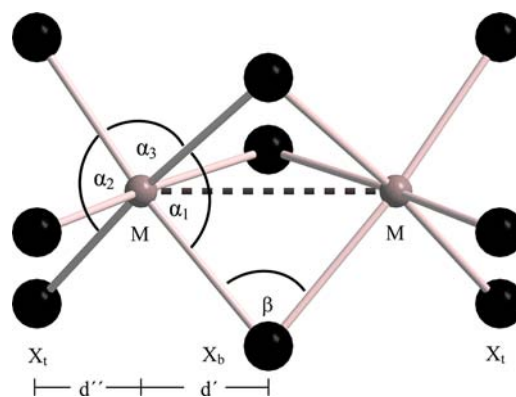
	$In_3Ti_2Cl_9$	$K_3Ti_2Cl_9$	$Rb_3Ti_2Cl_9$	$Cs_3Ti_2Cl_9$	$In_3Ti_2Br_9$	$K_3Ti_2Br_9$	$Rb_3Ti_2Br_9$	$Cs_3Ti_2Br_9$
reference	ref 24	this work	ref 26	ref 25	ref 15	this work	ref 14	ref 14
space group	$P6_3/mmc$	$P6_3/m$	$P6_3/mmc$	$P6_3/mmc$	$P6_3/mmc$	$P6_3/m$	$P6_3/mmc$	$P6_3/mmc$
a [Å]	7.058	7.073	7.119	7.322	7.382	7.428	7.520	7.656
c [Å]	17.291	17.544	17.647	17.998	18.139	18.382	18.724	18.958
V [Å ³]	746.1	760.1	774.7	835.8	856.0	878.5	916.9	962.4
c/a	2.450	2.480	2.479	2.458	2.457	2.474	2.490	2.476
Ti–Ti	3.016	3.108	3.146	3.215	3.145	3.281	3.364	3.434
Ti– X_b	2.473	2.509	2.511	2.524	2.618	2.654	2.684	2.698
Ti– X_t	2.353	2.352	2.341	2.348	2.507	2.495	2.511	2.512
X_b –Ti– X_b (α_1)	86.6	85.7	84.9	83.8	87.7	85.8	84.9	83.8
X_t –Ti– X_t (α_2)	93.1	94.4	94.6	95.0	92.6	94.7	94.4	94.9
X_b –Ti– X_t (α_3)	90.1	89.4	90.0	90.3	89.9	89.2	90.1	90.4
Ti– X_b –Ti (β)	75.2	76.5	77.6	79.1	73.8	76.4	77.6	79.0
d'/d''	1.175	1.244	1.270	1.305	1.137	1.246	1.262	1.299
Ti– X_b /Ti– X_t	1.051	1.064	1.073	1.075	1.044	1.064	1.069	1.074

Table 3. Selected Distances (Å) and Angles (deg) of $In_4Ti_3Br_{12}$

Ti1–Br1	2.6238(7) 6×	Br1–Ti1–Br1	88.20(2)°
Ti2–Br1	2.602(1) 3×	Br1–Ti1–Br1	91.80(2)°
Ti2–Br2	2.546(1) 3×	Br1–Ti2–Br1	90.19(2)°
Ti1–Ti2	3.086(1) 2×	Br1–Ti2–Br1	89.14(5)°
		Br2–Ti2–Br2	90.47(6)°
In1–Br2	3.242(1) 3×	In2–Br2	3.422(1) 3×
In1–Br1	3.746(1) 6×	In2–Br2	3.724(1) 6×
In1–Br1	4.296(1) 3×	In2–Br1	4.036(1) 3×

isolated face-sharing double-octahedra $[M_2X_9]^{3-}$. Because of the short distances of the M -atoms these units are excellent model systems for the investigation of M – M interactions⁵ by different means, for example spectroscopic⁶ and magnetic properties,⁷ inelastic neutron scattering,⁸ and theoretical calculations.⁹ Type and extent of the M – M interaction mainly depend on the size and d-configuration of the M -cation (no bonding interaction for cations with d^0 - and d^6 -configuration, that is, Sc^{3+} , Y^{3+} , Rh^{3+} , Ir^{3+} , and an intermediate situation for configurations d^1 – d^5). In a simple picture there is a “competition” between electrostatic repulsion, direct M – M bonding, and an exchange coupling via the bridging ligands. The interaction depends on absolute and relative sizes of A and X , too. This has an impact on the geometry of the $[M_2X_9]^{3-}$ dimer which was first discussed by Cotton and Ucko.²³ With reference to the geometry of an idealized (i.e., undistorted) dioctahedral unit, they defined the angles α_1 (X_t – M – X_t), α_2 (X_b – M – X_t), α_3 (X_b – M – X_b), and β (M – X_b – M), and the distances d' and d'' (distance of M to the triangle of X_b and X_t , respectively, see Figure 4). Idealized values for these parameters are $\alpha_1 = \alpha_2 = \alpha_3 = 90^\circ$, $\beta = 70.5^\circ$, and $d'/d'' = 1$.

Table 2 gives an overview on the geometrical parameters in $[Ti_2X_9]^{3-}$ dimers. As expected, all distances increase with the size of the halide anions. Furthermore, most of the distances are reduced for smaller A^+ cations. The results for the K compounds continue the tendency for the Rb and Cs representatives. According to the values of the unit cell volumes In^+ is the smallest cation in the series and, therefore, the shortest Ti–Ti distances are observed for the In-compounds. In general, the geometrical parameters of the $[M_2X_9]^{3-}$ dimer indicate an “elongation” along the c -axis. The deviation from the idealized geometry (β , d'/d'') is significantly smaller for the indium compounds.

Figure 4. Detailed geometry of a M_2X_9 dimer.

A second point of discussion on $A_3M_2X_9$ compounds results from the underlying perovskite structure which bases on a closest packing of A^+ cations and halide anions. This requires a suitable ratio of the ionic radii, which is quantified by the Goldschmidt condition $r_X + r_A = \sqrt{2}(r_M + r_X)$. Accordingly, distortions are likely for small A^+ (i.e., K^+ , In^+) and large M^{3+} (for 3d-metals Ti^{3+}). The A – X distances of the $P6_3/mmc$ structures with $A = Rb$, Cs show that the coordination of $A1$ is nearly regular, while for $A2$ differences of up to 10% are observed. In contrast, the coordination of K^+ in the $P6_3/m$ structure is strongly distorted with difference of up to 18% (Figure 5a). For K1 3 short, 6 medium, and 3 long distances are observed, and K2 has 3 + 3 short and 3 + 3 long ones. The average distances for K1 and K2 are nearly the same ($K_3Ti_2Cl_9$: 3.52/3.58 Å; $K_3Ti_2Br_9$: 3.74/3.77 Å). Obviously, K^+ is too small for a more regular coordination. The adjustment is achieved by a rotation of the $[Ti_2X_9]^{3-}$ unit parallel to the c -axis. Thus, the mirror plane perpendicular to the a -axis is removed, and the symmetry is reduced from $P6_3/mmc$ to $P6_3/m$. This rotation can occur in opposite directions which explains the presence of merohedral twins. Probably, the $P6_3/mmc$ structure occurs as high temperature modification as it was observed for $K_3Mo_2Cl_9$.²⁷ Beekhuizen reports for $K_3Ti_2Cl_9$ a first order transition at 244 °C.²⁶ According to the greater size difference for K/Br in comparison to K/Cl the rotation angle of the dimer is 5.7° in $K_3Ti_2Cl_9$ and 7.5° in $K_3Ti_2Br_9$. The six equatorial K– X distances which would be equal by symmetry in $P6_3/mmc$

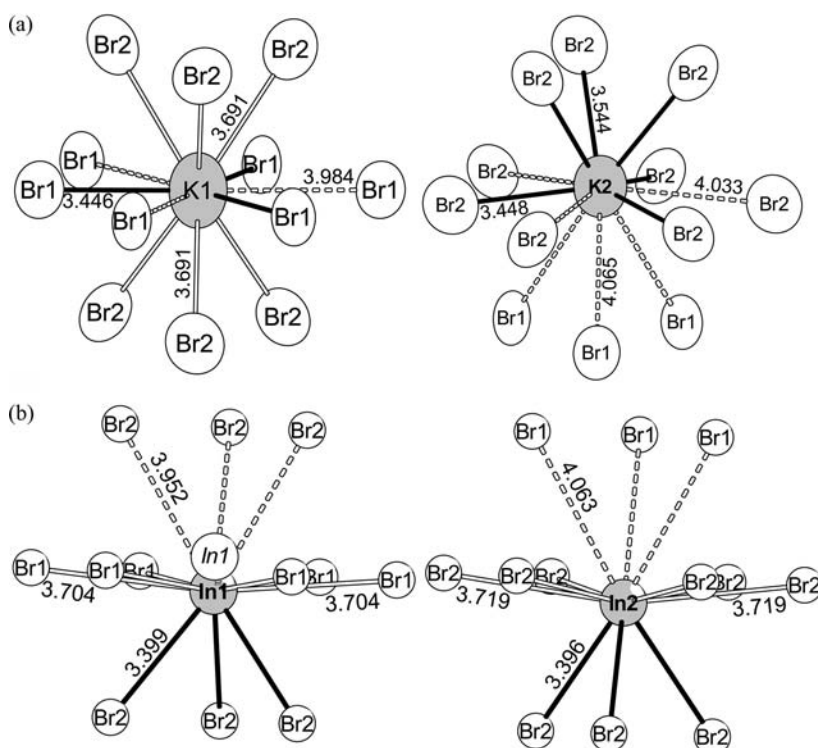


Figure 5. Coordination polyhedra of A^+ cations in (a) $K_3Ti_2Br_9$ (K1 and K2 have $\bar{6}$ and 3 site symmetries, respectively) and (b) $In_3Ti_2Br_9$ (In1 and In2 have $\bar{6}m2$ and $3m$ site symmetries, respectively); ellipsoids ($K_3Ti_2Br_9$) with 80% probability.

differ now by 10% ($K_3Ti_2Cl_9$) and 14% ($K_3Ti_2Br_9$), respectively.

Interestingly, a comparable but different symmetry reduction is observed for the In-compounds (Figure 5b). In^+ is the smallest A^+ cation in the series. The In–X distances are split into 3 short, 6 medium, and 3 long ones with length differences up to 19%. This is achieved by a shift along the c -axis of In1 by 0.27 Å/0.33 Å and In2 by 0.42 Å/0.45 Å for $X = Cl/Br$, respectively. For In1 the shift results in a split position. According to our experience with $K_3Ti_2Cl_9$ and $K_3Ti_2Br_9$, the formation of merohedral twins might be an explanation for the large displacement parameters in $In_3Ti_2Br_9$. Therefore, crystals of $In_3Ti_2Br_9$ were reinvestigated, but there was no signature for a symmetry reduction to $P6_3/m$, even at 150 K.

Symmetry reductions were also observed for the divalent Ti-halides $ATiX_3$ ($A = K, Rb, Cs$; $X = Cl, Br, I$; ref 4 and references therein). For $A = Cs$ the hexagonal perovskite of $BaNiO_3$ structure with space group $P6_3/mmc$ is observed, while the symmetry of the potassium compounds is reduced to $P6_3$ and its unit cell volume enlarged by a factor of 3.

As already pointed out, the compounds with dioctahedral $[M_2X_9]^{3-}$ dimers are model compounds for the M – M interaction in trihalides MX_3 with chain structure of face-sharing octahedra.^{11,12} Titanium is the only 3d-metal which forms this chain structure. Meyer has pointed out that TiI_3 and β - $TiBr_3$ ^{4,28} behave like 1D metals at elevated temperatures and show a Peierls transition to a semiconductor at lower temperatures. This transition is connected to alternating M – M distances. The values for β - $TiBr_3$ are 3.045 Å (HT-phase) and 2.923/3.157 Å (LT-phase). According to band structure calculations and geometrical parameters the short distances in the LT-forms are considered to be direct Ti–Ti bonds. A comparison to the geometry of the isolated $Ti_2Br_9^{3-}$ units shows much weaker bonding interactions in the $Ti_2Br_9^{3-}$ units.

$In_4Ti_3Br_{12}$. Structure. Similar to $In_3Ti_2Br_9$, the crystal structure of $In_4Ti_3Br_{12}$ is based on a closest packing of In^+ and Br^- ions with Ti cations in 3/4 of the octahedral voids formed by bromine (Figure 6). The layer sequence is

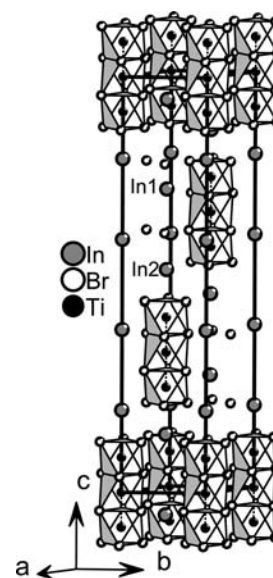


Figure 6. Crystal structure of $In_4Ti_3Br_{12}$.

ABABCACABCBC or $(h\bar{h}cc)_3$, which is known from the 12R- (or 12L-) perovskites.^{1,2,29} Because the free octahedral voids are those between the cubic sequence the resulting structural units are linear $[Ti_3Br_{12}]^{4-}$ trimers built from face-sharing octahedra (Figure 7). According to the characteristics of closest sphere packings there are two different In^+ sites, both with CN 12. In1 is located in the hexagonal sequence with

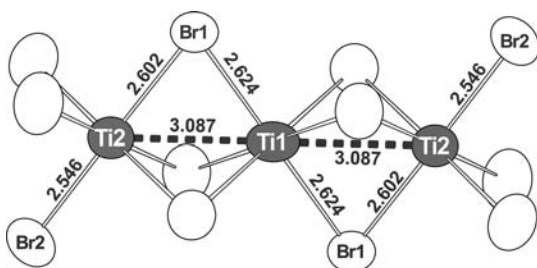


Figure 7. Geometry of $[\text{Ti}_3\text{Br}_{12}]^{4-}$ trimers in $\text{In}_4\text{Ti}_3\text{Br}_{12}$; ellipsoids with 80% probability.

“anti”-cuboctahedral coordination and In2 in the cubic sequence with a cuboctahedral coordination (Figure 8). According to our knowledge $\text{In}_4\text{Ti}_3\text{Br}_{12}$ represents a new type of structure.

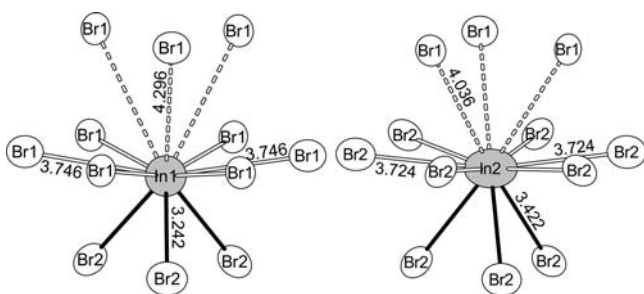


Figure 8. Coordination polyhedra of In^+ cations in $\text{In}_4\text{Ti}_3\text{Br}_{12}$; ellipsoids with 80% probability, both sites have $3m$ point symmetry.

The most prominent feature of $\text{In}_4\text{Ti}_3\text{Br}_{12}$ is the $\text{Ti}_3\text{Br}_{12}^{4-}$ unit. Similar to the dioctahedra $[\text{Ti}_2\text{Br}_9]^{3-}$ in $\text{In}_3\text{Ti}_2\text{Br}_9$ (Ti–Br: 2.507/2.618 Å) the terminal Ti–Br distances are shorter than the bridging ones, but the difference is less significant (2.546/2.602/2.624 Å). Accordingly, the “central” distances are the longest. In general, the deviation from regular TiBr_6 octahedra decreases from $\text{In}_3\text{Ti}_2\text{Br}_9$ to $\text{In}_4\text{Ti}_3\text{Br}_{12}$. Despite the longer bridging Ti–Br distances the Ti–Ti distance in $[\text{Ti}_3\text{Br}_{12}]^{4-}$ is shorter (3.087 Å) than in $\text{In}_3\text{Ti}_2\text{Br}_9$ (3.145 Å). This is in line with the stronger antiferromagnetic coupling (see below).

The structural features suggest that the $[\text{Ti}_3\text{Br}_{12}]^{4-}$ anion be described as a mixed-valent species $\text{Ti}(\text{III})\text{–Ti}(\text{II})\text{–Ti}(\text{III})$ and interactions $\text{Ti}(d^1)\text{–Ti}(d^2)\text{–Ti}(d^1)$. This fits well to the Ti–Br distances of divalent (TiBr₂: 2.65 Å;³⁰ RbTiBr₃: 2.675 Å⁴) and trivalent ($\alpha\text{-TiBr}_3$: 2.583 Å;³¹ Rb₃TiBr₆: 2.593 Å²⁶) Ti-bromides. $\text{In}_4\text{Ti}_3\text{Br}_{12}$ is closely related to the monoclinic structure of $\text{K}_4\text{Ti}_3\text{Br}_{12}$.²⁰ This is a distorted variant of a 12R-perovskite and contains mixed-valent $[\text{Ti}_3\text{Br}_{12}]^{4-}$ units, too.

The interpretation of the Ti–Ti distance in $\text{In}_4\text{Ti}_3\text{Br}_{12}$ is more difficult. It is longer than in elemental Ti (2.894 Å), but

the shortest in condensed octahedral TiBr_6 units (Table 4) with the exception of $\text{LT-}\beta\text{-TiBr}_3$. Because of geometrical reasons the discussion of the interaction cannot be limited to the Ti–Ti distances. The extension of face-sharing units restricts the ability of the metal atoms to react on a repulsive interaction by an off-center shift. But in agreement to the magnetic properties we assume a weak bonding interaction.

The discussion of the Ti–Ti interaction in $[\text{Ti}_2\text{Br}_9]^{3-}$ and $[\text{Ti}_3\text{Br}_{12}]^{4-}$ should include the similar systems of Ru and Mo. The magnetic measurements show strong antiferromagnetic coupling for all systems $[\text{M}_2\text{X}_9]^{3-}$, $[\text{M}_3\text{X}_{12}]^{3-}$, and $[\text{M}_3\text{X}_{12}]^{4-}$ ($M = \text{Ti, Mo, Ru; X} = \text{Cl, Br, I}$). However, the interaction seems to be different for Ti and the 4d metals.

The situation is quite clear for the dimers $[\text{M}_2\text{X}_9]^{3-}$. According to the short $M\text{–}M$ distances, the strongly reduced magnetic moments, and the reduction of the $M\text{–}X_b\text{–}M$ angle, a strong direct $M\text{–}M$ bond is obvious for $M = \text{Mo}$ and Ru , in contrast to the Ti representatives. ($\text{Cs}_3\text{Mo}_2\text{Cl}_9$: 2.665 Å, 64.5°;³⁴ $\text{Cs}_3\text{Mo}_2\text{Br}_9$: 2.816 Å, 64.9°;^{11,34} $\text{Cs}_3\text{Mo}_2\text{I}_9$: 2.939 Å, 63.4°;¹¹ $\text{Cs}_3\text{Ru}_2\text{Cl}_9$: 2.725 Å, 69.5°;³⁵ $\text{Cs}_3\text{Ru}_2\text{Br}_9$: 2.835 Å, 68.4°;¹¹ $\text{Cs}_3\text{Ru}_2\text{I}_9$: 2.918 Å, 66.1°¹¹).

For the trimers the dependence of the $M\text{–}M$ distances is ambiguous. For $[\text{Ru}_3\text{Cl}_{12}]^{4-}$ with two Ru(III) and one Ru(II) Cotton et al. have explained the Ru–Ru distance of 2.805 Å (Ru–Cl_b–Ru: 72.4°) as a 2e–3c bond (i.e., bond order 0.5).^{16a,b} As a consequence the additional electron for $[\text{Ru}_3\text{Cl}_6(\text{PR}_3)_6]^+$ units with two Ru(II) and one Ru(III) enlarges the distance to 3.08 Å (Ru–Cl_b–Ru: 78°) because it is localized in an antibonding orbital.^{16c} For the $\text{Mo}_3\text{I}_{12}^{3-}$ unit the situation is in between of $[\text{Ru}_3\text{Cl}_{12}]^{4-}$ and $[\text{Ti}_3\text{Br}_{12}]^{4-}$ despite the strong bonding interaction in $[\text{Mo}_2\text{X}_9]^{3-}$ units. Mo–Mo distance (3.26 Å) and Mo–I_b–Mo angle (71.3°) are significantly larger than in $[\text{Mo}_2\text{I}_9]^{3-}$, but still indicate a direct Mo–Mo bond.

While the Ti–Ti distances in the trimers are shorter than in the dimers this is reversed for Mo and Ru. Even the $M\text{–}M$ distances of the MX_3 HT-phases follow this tendency (MoI_3 : 3.205 Å,¹¹ $\beta\text{-RuCl}_3$: 2.828 Å^{12b}).

Magnetic Properties. Magnetic susceptibility measurements of $\text{In}_4\text{Ti}_3\text{Br}_{12}$ are shown in Figure 9. The $1/\chi$ versus T curve displays a linear behavior above 100 K. A fit between 108 and 298 K, cf. the dashed line in Figure 9, yields a Weiss constant of $-1216(6)$ K ($= -845$ cm⁻¹). The huge negative Weiss constant indicates strong antiferromagnetic interactions in $\text{In}_4\text{Ti}_3\text{Br}_{12}$. The temperature dependence of μ_{eff}^2 per Ti ion in $\text{In}_4\text{Ti}_3\text{Br}_{12}$ is shown in Figure 10. The steep slope over the whole temperature range confirms the strong antiferromagnetic interactions. Its value is far below the spin only value of 4.67 μ_{B}^2 per Ti ion, a number which results from the average of two Ti^{3+} ($\mu_{\text{eff}}^2 = 3 \mu_{\text{B}}^2$) and one Ti^{2+} ($\mu_{\text{eff}}^2 = 8 \mu_{\text{B}}^2$) in $\text{In}_4\text{Ti}_3\text{Br}_{12}$.

Table 4. Geometrical Parameters in Ti-Bromides

	$\text{In}_4\text{Ti}_3\text{Br}_{12}$	$\text{In}_3\text{Ti}_2\text{Br}_9$	$\text{K}_4\text{Ti}_3\text{Br}_{12}$	$\text{K}_3\text{Ti}_2\text{Br}_9$	KTiBr_3	RbTiBr_3	CsTiBr_3
reference	this work	ref 15	ref 20	this work	ref 32	ref 32	ref 33
d (Ti–Ti) [Å]	3.087	3.144	3.20	3.281	3.16–3.17 ^a	3.158	3.185
d (Ti–Br _t) [Å]	2.546	2.507		2.495	2.56–2.72 ^a	2.675 ^b	2.683 ^b
d (Ti–Br _b) [Å]	2.624/2.602	2.618		2.654	2.56–2.72 ^a	2.675 ^b	2.683 ^b
Ti–Br _b –Ti [deg]	72.4	73.4		76.4	73.0	73.4	72.7
volume in [Å ³] per formula unit	579.6	426.3	595.6	439.3			

^aSymmetry reduced. ^bEqual by symmetry.

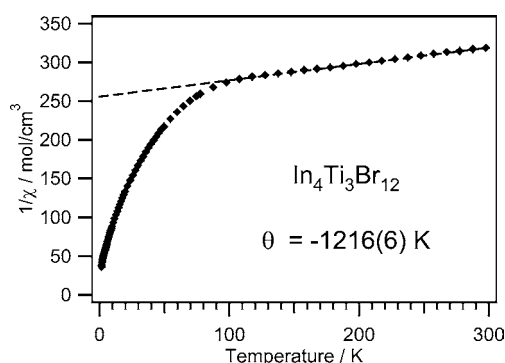


Figure 9. Reciprocal magnetic susceptibility of $\text{In}_4\text{Ti}_3\text{Br}_{12}$ measured at 500 Oe. The dashed line shows a Curie–Weiss fit to the data between 108 and 298 K.

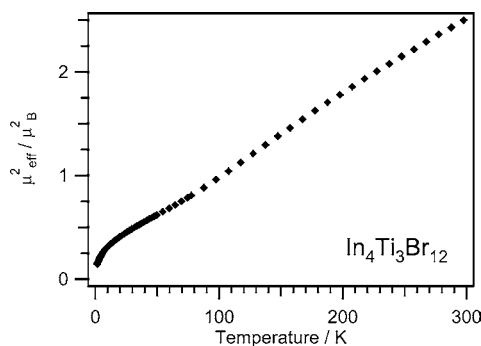


Figure 10. μ_{eff}^2 per Ti ion of $\text{In}_4\text{Ti}_3\text{Br}_{12}$.

The magnetic measurements indicate strong antiferromagnetic interactions between the Ti^{3+} – Ti^{2+} – Ti^{3+} ions in the linear $[\text{Ti}_3\text{Br}_{12}]^{4-}$ trimer. From a chemical point of view, the antiferromagnetic interactions correspond to two (weak) single bonds which couple the 4 electrons of the d^1 – d^2 – d^1 titanium trimer. Similar situations were observed in several titanium halides containing Ti^{3+} and/or Ti^{2+} cations. $\text{Cs}_3\text{Ti}_2\text{Cl}_9$ and $\text{Rb}_3\text{Ti}_2\text{Br}_9$ ^{6b} contain $[\text{Ti}_2\text{X}_9]^{3-}$ dimers of Ti^{3+} ions with strong antiferromagnetic coupling in agreement to the values of Briat et al. ($\text{Cs}_3\text{Ti}_2\text{Cl}_9$; -525 cm^{-1}).^{6a} Strong interactions between Ti^{2+} ions were also observed in the triangular Ti trimers of $\text{Na}_2\text{Ti}_3\text{Cl}_8$.³⁶

A strong antiferromagnetic coupling of $J = -618 \text{ K}$ (-430 cm^{-1}) was also observed for $\text{In}_3\text{Ti}_2\text{Br}_9$ ¹⁵ but in agreement to the shorter Ti–Ti distances the coupling in $\text{In}_4\text{Ti}_3\text{Br}_{12}$ is stronger.

Relation of $\text{In}_4\text{Ti}_3\text{Br}_{12}$ to $\text{K}_4\text{Ti}_3\text{Br}_{12}$ and Other Linear Trimers. Despite the close similarity of the crystal structures, the subtle differences between $\text{In}_3\text{Ti}_2\text{Br}_9$ and $\text{K}_3\text{Ti}_2\text{Br}_9$ are continued for $\text{In}_4\text{Ti}_3\text{Br}_{12}$ and $\text{K}_4\text{Ti}_3\text{Br}_{12}$. First, Ti–Ti distances and Ti–Br_b–Ti angles are significantly smaller for the In-compounds. Second, the anomaly of the In^+ volume shows up for $\text{In}_4\text{Ti}_3\text{Br}_{12}$, too. Third, the adoption to the size requirements of K^+ and In^+ by symmetry reduction takes place again in different ways. The monoclinic unit cell in $\text{K}_4\text{Ti}_3\text{Br}_{12}$ has a pseudohexagonal metric (ratio a/b close to $\sqrt{3}$), but the monoclinic angle β does not fit to the rhombohedral unit cell of $\text{In}_4\text{Ti}_3\text{Br}_{12}$ (i.e., projection of c on a is far away from $1/3$ of a). A similar deviation was observed for 12 L-perovskites $\text{Ba}_3\text{LnRu}_3\text{O}_{12}$ ($\text{Ln} = \text{lanthanides}$).³⁷ Depending from the size of Ln a symmetry reduction to a monoclinic unit cell ($C2/m$) with pseudohexagonal metrics ($a/b \approx \sqrt{3}$, $\beta = 90.91^\circ$) occurs.

A similar transformation of the unit cell of $\text{K}_4\text{Ti}_3\text{Br}_{12}$ results in $\beta = 91.8^\circ$.

Linear trimeric units of solely trivalent cations are known for group 15 iodide complexes, that is, $[\text{Sb}_3\text{I}_{12}]^{3-}$ and $[\text{Bi}_3\text{I}_{12}]^{3-}$.^{38,39} In these examples the distances between the ns^2 cations Sb^{3+} and Bi^{3+} are much longer ($>4 \text{ \AA}$).

The trimers in $\text{In}_4\text{Ti}_3\text{Br}_{12}$ continue the series of mixed-valent transition metal halides. Another example is $[\text{Pt}_3\text{Br}_{12}]^{2-}$ with two Pt(IV)Br_6 octahedra connected by a square-planar (Pt(II)Br_4) unit.⁴⁰ According to the electronic situation ($\text{Pt(IV): } d^6$; $\text{Pt(II): } d^8$) and a Pt–Pt distance of 3.61 \AA , there is no Pt–Pt interaction expected. In $\text{Ba}_6\text{Pr}_3\text{I}_{19}$ there are trimers of face-sharing square antiprisms $[\text{Pr}_3\text{I}_{16}]^{9-}$.⁴¹ Here the Pr–Pr distances of 3.56 \AA are discussed as a significant $2e$ – $3c$ bond according to Extended-Hückel calculations and geometrical considerations (i.e., size of Pr cations).

Coordination and Ionic Radius of In^+ . The well-developed $3 + 6 + 3$ coordination of In^+ is observed for both indium sites (Figure 5b). The cuboctahedrally coordinated $\text{In}2$ has nearly the same splitting like In^+ in $\text{In}_3\text{Ti}_2\text{Br}_9$ ($\pm 10\%$). For $\text{In}1$ in the anticuboctahedral surrounding this splitting is even larger ($\pm 15\%$). The disorder of In^+ on different sites to achieve the typical $3 + 6 + 3$ splitting is not necessary for $\text{In}_4\text{Ti}_3\text{Br}_{12}$ because the site symmetry is $3m$ in both cases.

The description of In(I) as a monovalent cation In^+ is well-established as there exist several ionic compounds with monovalent indium.^{10,42} Nevertheless, no ionic radius on In^+ is given in the literature.^{1,2,43} From volume considerations a similarity to K^+ is obvious. First approaches are the perovskite-related structures of the In-compounds of the series $\text{A}_3\text{Ti}_2\text{X}_9$ and $\text{A}_4\text{Ti}_3\text{Br}_{12}$. But a more detailed view shows that the special character of In^+ as a ns^2 cation is still present. The increase of volume from an alkali chloride to a bromide is about 10 \AA^3 per formula unit ($\text{KCl: } 61.3 \text{ \AA}^3$; $\text{KBr: } 70.9 \text{ \AA}^3$; $\text{RbCl: } 71.2 \text{ \AA}^3$; $\text{RbBr: } 81.4 \text{ \AA}^3$). For the binary indium halides this increase is only about 4 \AA^3 ($\text{InCl: } 61.3 \text{ \AA}^3$; $\text{InBr: } 65.4 \text{ \AA}^3$). Similar tendencies are found for the ternaries $\text{A}_3\text{Ti}_2\text{X}_9$ ($\text{X} = \text{Cl, Br}$) (Table 2) and $\text{A}_4\text{Ti}_3\text{Br}_{12}$ ($\text{A} = \text{K, In}$) (Table 4) where the volume of In^+ in a surrounding of Br^- is smaller than expected. Nevertheless, the volume of In(I) compounds is the smallest one.

The “wobbly character” of In^+ was already described by Dronskowski^{15,44} and seems to depend significantly on the coordination number. For the isotopic series KMnBr_3 ⁴⁵/ InMnBr_3 and KFeBr_3 ⁴⁶/ InFeBr_3 (NH_4CdCl_3 -type) the volumes of the K compounds are slightly smaller ($553.1/572.4 \text{ \AA}^3$ vs $558.1/577.6 \text{ \AA}^3$). But despite the similar volume, there are significant differences between the lattice parameters.

CONCLUSIONS

Single crystals of $\text{K}_3\text{Ti}_2\text{Cl}_9$ and $\text{K}_3\text{Ti}_2\text{Br}_9$ were obtained by solid state reactions. The deviation from the idealized geometry (i.e., regular face-sharing dioctahedra) decreases with larger anions and smaller cations. In $\text{K}_3\text{Ti}_2\text{Cl}_9$ and $\text{K}_3\text{Ti}_2\text{Br}_9$ symmetry reductions occur by rotation of the $[\text{Ti}_2\text{X}_9]^{3-}$ units. This rotation results by geometrical reasons to optimize the coordination of K^+ and leads to merohedral twins. This is not the case for $\text{In}_3\text{Ti}_2\text{Br}_9$ despite its smaller volume.

The new compound $\text{In}_4\text{Ti}_3\text{Br}_{12}$ was obtained from InBr_3 and Ti. The rhombohedral crystal structure represents a new type of 12 L- (or 12R-)perovskite. It contains linear trimeric units $[\text{Ti}_3\text{Br}_{12}]^{4-}$ of face-sharing octahedra. The distances within the $[\text{Ti}_3\text{Br}_{12}]^{4-}$ unit and its geometrical features suggest the description as a mixed-valent system (Ti^{3+} – Ti^{2+} – Ti^{3+}) and a

weak bonding interaction between the Ti atoms. The strong antiferromagnetic coupling observed for the $[\text{Ti}_2\text{X}_9]^{3-}$ ($X = \text{Cl}, \text{Br}$) units is continued for trimeric units $[\text{Ti}_3\text{Br}_{12}]^{4-}$ in $\text{In}_4\text{Ti}_3\text{Br}_{12}$. In agreement to the shorter Ti–Ti distances compared to $\text{In}_3\text{Ti}_2\text{Br}_9$, the coupling constant is enlarged.

Although $\text{In}_3\text{Ti}_2\text{Br}_9$ and $\text{In}_4\text{Ti}_3\text{Br}_{12}$ fit perfectly to perovskite-related structures with a closest sphere packing made of cations A^+ and anions X^- , In^+ is not a simple monovalent cation. This becomes obvious by its unusual molar volume in comparison to K^+ and Rb^+ . As well the symmetry reduction is different from K^+ and related to the special situation of a ns^2 cation.

The structure of $\text{In}_4\text{Ti}_3\text{Br}_{12}$ continues the row of ordered defect perovskites. In a similar way as the ordered perovskites $A_2BB'X_6$ (cubic elpasolite structure, $Z = 4$, $Fm\bar{3}m^{1,2}$), $A_3B_2B'X_9$ ($Z = 2$, $P6_3/mmc$, sequence $(hcc)_2$, with B' in octahedral voids of the cubic sequence, for example, $\text{Ba}_3\text{MgRu}_2\text{O}_9^{47}$), and $A_4B_3B'X_{12}$ ($Z = 3$, $R\bar{3}m$; sequence $(hhcc)_3$, for example $\text{Ba}_4\text{ZrRu}_3\text{O}_{12}^{29}$) are representatives of stacking variants $A_{n+1}B_nB'X_{3n+3}$; there are defect perovskites with vacant sites \square for B' , that is, $A_{n+1}(B_n\square)X_{3n+3}$. Among them $n = 1$ represents the K_2PtCl_6 -type ($A_2(B,\square)X_6$), $n = 2$ corresponds to the $\text{Cs}_3\text{Cr}_2\text{Cl}_9$ structure, and $\text{In}_4\text{Ti}_3\text{Br}_{12}$ is now an example for $n = 3$.

Finally, the linear trimers $[\text{Ti}_3\text{Br}_{12}]^{4-}$ represent a less frequently realized variant of three interacting transition metals cations with octahedral coordination. Usually cyclic variants are found like in $\text{Na}_2\text{Ti}_3\text{Cl}_9$,³⁶ Ti_7X_{16} ($X = \text{Cl}, \text{Br}$),⁴⁸ Nb_3X_8 ($X = \text{Cl}, \text{Br}, \text{I}$),⁴⁹ $[\text{Mo}_3\text{Br}_{11}]^{2-}$,⁵⁰ $\text{Na}_3\text{W}_3\text{Cl}_{13}$,⁵¹ or ReX_3 ($X = \text{Cl}, \text{Br}, \text{I}$).⁵²

In general, this contribution also shows that low-valent ternary halides of titanium are interesting compounds for new structural features and model systems for metal–metal exchange interactions.

■ ASSOCIATED CONTENT

📄 Supporting Information

Tables 1 and 2 with the atomic positions and displacement parameters of $\text{A}_3\text{Ti}_2\text{X}_9$ and $\text{In}_4\text{Ti}_3\text{Br}_{12}$ compounds, respectively. This material is available free of charge via the Internet at <http://pubs.acs.org>.

■ AUTHOR INFORMATION

Corresponding Author

*E-mail: harald.hillebrecht@ac.uni-freiburg.de. Phone: 0049-761-203 6131. Fax: 0049-761-203 6102.

Notes

The authors declare no competing financial interest.

■ ACKNOWLEDGMENTS

This work was supported by Deutsche Forschungsgemeinschaft (Project Hi 632/3-1) and the Swiss National Science Foundation (Grant 200020-130266)

■ REFERENCES

- (1) Wells, A. F. *Structural Inorganic Chemistry*, 5th ed.; Oxford Press: Oxford, U.K., 1984.
- (2) Müller, U. *Anorganische Strukturchemie*, 5. Auflage; Verlag Teubner: Wiesbaden, Germany, 2006.
- (3) Wessel, G. J.; Ijdo, D. J. W. *Acta Crystallogr.* **1957**, *10*, 466–468.
- (4) Meyer, G.; Gloger, T.; Beekhuizen, J. *Z. Anorg. Allg. Chem.* **2009**, *635*, 1497–1509.
- (5) Summerville, R.; Hoffmann, R. *J. Am. Chem. Soc.* **1979**, *101*, 3821–3831.

- (6) (a) Briat, B.; Kahn, O.; Morgenstern-Badarau, I.; Rioval, R. C. *Inorg. Chem.* **1981**, *20*, 4193–4200. (b) Leuenberger, B.; Güdel, H. U.; Furrer, A. *Chem. Phys. Lett.* **1986**, *126*, 255–259. (c) Stranger, R. *Inorg. Chem.* **1990**, *29*, 5231–5237.

- (7) (a) Crouch, P.; Fowles, G. W. A.; Walton, R. A. *J. Chem. Soc. A* **1969**, 972–976. (b) Ginsberg, A. P. *J. Am. Chem. Soc.* **1980**, *102*, 111–117. (c) Leuenberger, B.; Güdel, H. U. *Inorg. Chem.* **1986**, *25*, 181–184. (d) Stranger, R.; Smith, P. W.; Grey, I. E. *Inorg. Chem.* **1989**, *28*, 1271–1278.

- (8) (a) Leuenberger, B.; Güdel, H. U.; Fischer, P. *Phys. Rev. Lett.* **1985**, *55*, 2983–2986. (b) Leuenberger, B.; Briat, B.; Canit, J.-C.; Furrer, A.; Fischer, P.; Güdel, H. U. *Inorg. Chem.* **1986**, *25*, 2930–2935. (c) Leuenberger, B.; Güdel, H. U.; Fischer, P. *J. Solid State Chem.* **1986**, *64*, 90–101. (d) Leuenberger, B.; Güdel, H. U.; Kjems, J. K.; Petitgrand, D. *Inorg. Chem.* **1985**, *24*, 1035–1038.

- (9) (a) Leuenberger, B.; Güdel, H. U. *Mol. Phys.* **1984**, *51*, 1–20. (b) Stranger, R.; McGrady, J. E.; Lovell, T. *Inorg. Chem.* **1998**, *37*, 6795–6806. (c) Cavigliasso, G.; Stranger, R. *Inorg. Chem.* **2004**, *43*, 2368–2378. (d) Cavigliasso, G.; Lovell, T.; Stranger, R. *Dalton Trans.* **2006**, 2017–2025.

- (10) Pardoe, J. A. J.; Downs, A. J. *Chem. Rev.* **2007**, *107*, 2–45.

- (11) Hillebrecht, H. Ph.D. Thesis, University Freiburg, Freiburg, Germany, 1991.

- (12) (a) Hillebrecht, H.; Rotter, H. W.; Thiele, G. *Z. Kristallogr. Suppl.* **1989**, *2*, 448. (b) Hillebrecht, H.; Ludwig, Th.; Thiele, G. *Z. Anorg. Allg. Chem.* **2004**, *630*, 2199–2204.

- (13) (a) Brosset, C. *Mineral. Geol. A* **1935**, *12*, 8. (b) Watson, W. H.; Waser, J. *Acta Crystallogr.* **1958**, *11*, 689–691.

- (14) Hartwig, S. Ph.D. Thesis, University Bayreuth, Bayreuth, Germany, 2003.

- (15) Dronskowski, R. *Chem.—Eur. J.* **1995**, *1*, 118–123.

- (16) (a) Bino, A.; Cotton, F. A. *J. Am. Chem. Soc.* **1980**, *102*, 608–611. (b) Bursten, B. E.; Cotton, F. A.; Fang, A. *Inorg. Chem.* **1983**, *22*, 2127–2133. (c) Cotton, F. A.; Matusz, M.; Torralba, R. C. *Inorg. Chem.* **1989**, *28*, 1516–1520. (d) Cotton, F. A.; Torralba, R. C. *Inorg. Chem.* **1991**, *30*, 3293–3304. (e) Cotton, F. A.; Torralba, R. C. *Inorg. Chem.* **1991**, *30*, 4386–4391.

- (17) Delphin, W. H.; Wentworth, R. A. D.; Matson, M. S. *Inorg. Chem.* **1974**, *13*, 2552–2555.

- (18) Fettinger, J. C.; Gordon, J. C.; Mattamana, S. P.; O'Connor, C. J.; Poli, R.; Salem, G. *Inorg. Chem.* **1996**, *35*, 7404–7412.

- (19) Cavigliasso, G.; Stranger, R. *Inorg. Chem.* **2008**, *47*, 3072–3083.

- (20) Jongen, L.; Meyer, G. *Z. Anorg. Allg. Chem.* **2004**, *630*, 1732.

- (21) XAREA, XSHAPE, XRED Programs; Stoe Cie.: Darmstadt, Germany.

- (22) Sheldrick, G. M. *SHELXTL program package*; University of Göttingen: Götting, Germany, 1997.

- (23) Cotton, F. A.; Ucko, D. A. *Inorg. Chim. Acta* **1972**, *6*, 161–172.

- (24) Bajan, B.; Meyer, H.-J. *Z. Kristallogr.* **1996**, *211*, 817.

- (25) Gloger, T.; Hinz, D. J.; Meyer, G.; Lachgar, A. *Z. Kristallogr.* **1996**, *211*, 821.

- (26) Beekhuizen, J. Ph.D. Thesis, University Köln, Cologne, Germany, 2006.

- (27) Zickelbein, W. Ph.D. Thesis, University Münster, Münster, Germany, 1978.

- (28) Gloger, T. Ph.D. Thesis, University Köln, Cologne, Germany, 1998.

- (29) DeVreugd, C. H.; Zandbergen, H. W.; Ijdo, D. J. W. *Acta Crystallogr., Sect. C* **1984**, *40*, 1987–1989.

- (30) Ehrlich, P.; Gutsche, W.; Seifert, H. J. *Z. Anorg. Allg. Chem.* **1961**, *312*, 80–86.

- (31) Trojanov, S. I.; Rybakov, V. B.; Ionov, V. M. *Russ. J. Inorg. Chem.* **1990**, *35*, 494–498.

- (32) Jongen, L.; Gloger, T.; Beekhuizen, J.; Meyer, G. *Z. Anorg. Allg. Chem.* **2005**, *631*, 582–586.

- (33) Meyer, G.; Hinz, D. J.; Floerke, U. *Z. Kristallogr.* **1993**, *208*, 370.

- (34) Saillant, R.; Jackson, R. B.; Streib, W. E.; Folting, K.; Wentworth, R. A. D. *Inorg. Chem.* **1971**, *10*, 1453–1457.

- (35) Darriet, R. *Rev. Chim. Minér.* **1981**, *18*, 27–32.

- (36) Hinz, D. J.; Meyer, G.; Dedecke, T.; Urland, W. *Angew. Chem.* **1995**, *107*, 97–99; *Angew. Chem., Int. Ed. Engl.* **1995**, *34*, 71–73.
- (37) Shimoda, Y.; Doi, Y.; Hinatsu, Y. *Chem. Mater.* **2008**, *20*, 4512–4518.
- (38) Borgsen, B.; Weller, F.; Dehnicke, K. *Z. Anorg. Allg. Chem.* **1991**, *596*, 55.
- (39) Geiger, U.; Wade, E.; Wang, H. H.; Williams, J. M. *Acta Crystallogr., Sect. C* **1990**, *46*, 1547.
- (40) Hillebrecht, H.; Thiele, G.; Hollmann, P.; Preetz, W. *Z. Naturforsch. B* **1992**, *47*, 1099–1104.
- (41) Gerlitzki, N.; Mudring, A.-V.; Meyer, G. *Z. Anorg. Allg. Chem.* **2005**, *631*, 381–384.
- (42) Villars, P.; Cenzual, K. *Pearson's Crystal Data*, Release 2009/2010; ASM International: Materials Park, OH, 2009.
- (43) Shannon, R. D. *Acta Crystallogr., Sect. A* **1976**, *32*, 751–767.
- (44) (a) Dronskowski, R. *Inorg. Chem.* **1994**, *33*, 5927–5933.
(b) Dronskowski, R. *Inorg. Chem.* **1994**, *33*, 6201–6212.
- (45) Seifert, H.-J.; Dau, E. *Z. Anorg. Allg. Chem.* **1972**, *391*, 302–312.
- (46) Gurewitz, E.; Shaked, H. *Acta Crystallogr., Sect. B* **1982**, *38*, 2771–2775.
- (47) Donohue, P. C.; Katz, L.; Ward, R. *Inorg. Chem.* **1966**, *5*, 339–342.
- (48) Krebs, B.; Henkel, G. *Z. Anorg. Allg. Chem.* **1981**, *474*, 149–156.
- (49) (a) von Schnering, H.-G.; Wöhrle, H.; Schäfer, H. *Naturwissenschaften* **1961**, *48*, 159. (b) Simon, A.; von Schnering, H.-G. *J. Less-Common Met.* **1966**, *11*, 31–46.
- (50) Parakevopoulou, P.; Makedonas, C.; Psaroudakis, N.; Mitsolpoulou, C. A.; Floros, G.; Seressioti, A.; Ioannou, M.; Sanakis, Y.; Rath, N.; Garcia, C. J. G.; Stavropoulos, P.; Mertis, K. *Inorg. Chem.* **2010**, *49*, 2068–2076.
- (51) Weisser, M.; Tragl, S.; Meyer, H.-J. *Z. Anorg. Allg. Chem.* **2006**, *632*, 1885–1889.
- (52) (a) Cotton, F. A.; Mague, J. T. *Inorg. Chem.* **1964**, *3*, 1402–1407. (b) Jung, B.; Erhardt, H.; Meyer, G. *Z. Anorg. Allg. Chem.* **1991**, *603*, 49–56. (c) Bennett, M. J.; Cotton, F. A.; Foxman, B. M. *Inorg. Chem.* **1968**, *7*, 1563–1569.